Chemical Science

ROYAL SOCIETY OF CHEMISTRY

EDGE ARTICLE

View Article Online
View Journal | View Issue

Cite this: *Chem. Sci.*, 2025, **16**, 2222

All publication charges for this article have been paid for by the Royal Society of Chemistry

Received 7th October 2024
Accepted 9th November 2024

DOI: 10.1039/d4sc06782g

rsc.li/chemical-science

Annulated carbocyclic gallylene and bis-gallylene with two-coordinated Ga(I) atoms†

Arne Merschel, Shkelqim Heda, Yury V. Vishnevskiy, Beate Neumann, Hans-Georg Stammler and Rajendra S. Ghadwal *

The first carbocyclic gallylene [(ADC)$_2$Ga(GaI$_2$)] and bis-gallylene [(ADC)Ga]$_2$ (ADC = PhC{N(Dipp)C}$_2$; Dipp = 2,6-iPr$_2$C$_6$H$_3$) featuring a central C$_4$Ga$_2$ ring annulated between two 1,3-imidazole rings are prepared by KC$_8$ reductions of [(ADC)GaI$_2$]$_2$. Treatment of [(ADC)Ga]$_2$ with Fe$_2$(CO)$_9$ affords complex [(ADC)GaFe(CO)$_4$]$_2$ in which each Ga(I) atom serves as a two-electron donor. [(ADC)Ga]$_2$ activates white phosphorus (P$_4$) and the C$_{sp^2}$–F bond of aryl fluorides (ArF) to yield compounds [(ADC)Ga(P$_4$)]$_2$ and *cis*-/*trans*-[(ADC)GaF(Ar)]$_2$, respectively. [(ADC)Ga]$_2$ undergoes oxidation with (Me$_2$S)AuCl to give [(ADC)GaCl$_2$]$_2$, while with PhN=NPh it forms [1 + 4]-cycloaddition product [(ADC)GaN(Ph)N=C$_6$H$_5$]$_2$ by the dearomatization of one of the phenyl rings.

Introduction

The isolation of first crystalline N-heterocyclic carbene (NHC) by Arduengo[1] prompted the search for stable carbene analogues of heavier Group 13 and 14 elements, *i.e.* metallylenes.[2] Like carbenes, metallylenes are in general highly reactive species. The first Al(I) and Ga(I) compounds were reported as tetrameric species (**I**-E)$_4$ (ref. 3) and [GaC(SiMe$_3$)$_3$]$_4$ (ref. 4) in the solid state (Fig. 1). In 1999, Schmidbaur reported the first anionic Ga(I) compound **II** (R = *t*Bu).[5] Subsequently, serval other anionic as well as neutral compounds with a two-coordinated Ga(I) or Al(I) atom were reported.[2,6] In 2000, Roesky and Power independently reported the first aluminylene[7] and gallylene[8] compounds (**III**-E), respectively, based on a bulky β-diketiminate ligand. Over the past years, **III**-E have been extensively investigated to access a variety of Al/Ga-compounds with intriguing structures and properties.[6a] The fascinating chemistry of these species prompted further interests in the isolation of new thermally stable Group 13 metallylenes.[9] Among monocoordinated metallylenes, Power *et al.* reported the first Ga(I) species Ar(Me$_3$Si)NGa (Ar = 2,6-Mes$_2$C$_6$H$_3$; Mes = 2,4,6-Me$_3$C$_6$H$_2$) in 2006 (ref. 10) and the first Al(I) compound **IV**-E in 2020.[11] Subsequently, the research groups of Liu,[12] Hinz,[13] and Tan[14] reported monocoordinated Group 13 metallylene compounds using a bulky carbozole ligand. Very recently, Kretschmer and colleagues isolated a mono-coordinated Ga(I) compound.[15] Like singlet carbenes, Group 13 metallylenes are promising ligands in organometallic chemistry.[12,16] In general, most of the known examples of neutral as well as anionic metallylene species[9b,17] are based on chelating N-donor ligands.[2,6] The use of singlet carbenes for the stabilization of borylene species has been shown,[18] however, related heavier metallylenes remained rather scarce.[19] Like other main-group homonuclear heavier alkenes (*i.e.* for example the dimers of metallylenes),[20] digallenes may also be regarded as dimers of gallylenes.[10,21] Among three coordinated Ga(I) compounds, Lewis base-stabilized neutral[22] as well as dicationic[23] digallene compounds are known. We have shown the suitability of 1,3-imidazole-based anionic dicarbenes (ADCs) **V** in accessing a variety of low-valent main-group heterocycles.[24] Compounds **VI** featuring formally P(I),[25] As(I)[26] or Sb(I)[27] atoms are accessible as crystalline solids. Attempts to isolate the aluminylene species **VII** were unfortunately unsuccessful as it underwent C–H bond activation to yield an annulated Al(III) compound in 76% yield.[28] Herein, we report the first carbocyclic gallylene as well as bis-gallylene compounds (Schemes 1 and 2) as crystalline solids and showcase the reactivity of the bis-gallylene towards transition metal, white phosphorus, organofluorine, and azobenzene substrates.

Results and discussion

The starting Ga(III) hydride [(ADC)GaH$_2$]$_2$ (**3**) (ADC = PhC{N(Dipp)C}$_2$, Dipp = 2,6-iPr$_2$C$_6$H$_3$) was prepared by reacting freshly prepared LiGaH$_4$ and Li(ADC) (**2**)[29] as a colorless crystalline solid in 99% yield (Scheme 1). Compound **1** was synthesized by the direct C2-arylation of the corresponding NHC under nickel catalysis.[30] Compound **3** is stable under an inert gas (N$_2$ or Ar) atmosphere but slowly decomposes when

Molecular Inorganic Chemistry and Catalysis, Inorganic and Structural Chemistry, Center for Molecular Materials, Faculty of Chemistry, Universität Bielefeld, Universitätsstrasse 25, D-33615, Bielefeld, Germany. E-mail: rghadwal@uni-bielefeld.de; Web: http://www.ghadwalgroup.de

† Electronic supplementary information (ESI) available. CCDC 2334945, 2334948–2334953, 2379059 and 2379060. For ESI and crystallographic data in CIF or other electronic format see DOI: https://doi.org/10.1039/d4sc06782g

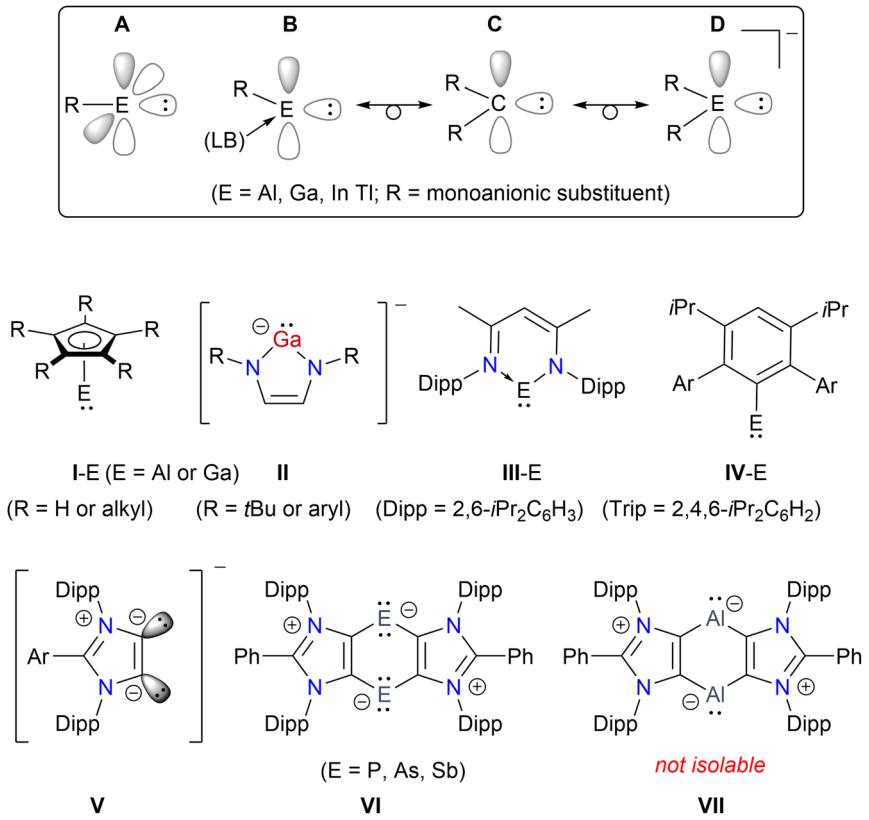

Fig. 1 Schematic illustration of Group 13 metallylenes (A), Lewis base (LB) stabilized metallylenes (B), singlet carbenes (C), and anionic species (D). Representative examples E(I) compounds (I-E–IV-E). Anionic dicarbene (ADC) V derived Group 15 heterocycles VI and a related transient Al(I) compound VII.

exposed to air. The ^{1}H and $^{13}C\{^{1}H\}$ NMR spectra of **3** exhibit well-resolved signals, which are fully consistent with the related aluminium species [(ADC)AlH_2].[31] The ^{1}H NMR spectrum of **3** shows a broad signal at 4.16 ppm for the GaH_2 moieties that is comparable with those of NHC-stabilized Ga(III) hydrides.[32] The FT-IR spectrum of **3** displays two characteristic bands at 1800 and 1830 cm^{-1} for the Ga–H stretching vibrations.[32,33] Treatment of **3** with methyl iodide (or iodine) at 80 °C affords the Ga(III) iodide **4** as a white solid. Compound **4** is insoluble in benzene and toluene but sparingly dissolves in chloroform. The ^{1}H and $^{13}C\{^{1}H\}$ NMR spectra of **4** show broad signals for the isopropyl groups, which is in line with an easily polarizable nature of iodides.[28] The $^{13}C\{^{1}H\}$ NMR signal for the gallium bound carbon atoms of **4** (164.0 ppm) is slightly downfield shifted compared to that of **3** (158.3 ppm).

The solid-state molecular structures of **3** and **4** (Fig. 2) show the expected atom connectivity.[34] The four-fold coordinated Ga(III) atoms in the C_4Ga_2 ring of **3** and **4** have a distorted tetrahedral coordination geometry. The C2–Ga1 (2.016(3) Å) and C4–Ga1 (2.015(3) Å) bond lengths of **3** are slightly smaller than those of NHC–Ga(III) hydrides (2.071(5) Å).[32] This may be attributed to the stronger σ-donor strength of mesoionic carbenes (iMICs) than NHCs.[35] The gallium bound hydrogen atoms of **3** were refined isotropically. The C2–Ga1–H (108.1(2)°) and C2–Ga1–Ha (113.7(2)°) bond angles of **3** are distinct. Like the Ga–H/Ha bond lengths in **3** (1.492(3)/1.574(3) Å), the Ga1–I1 (2.6117(1) Å) and Ga1–I2 (2.5230(1) Å) bond lengths of **4** are dissimilar (see below the NBO (Natural Bond Orbital) analysis). The I1 atom of **4** is situated out of the C_4Ga_2-ring plane, resulting the C3–C2–Ga1–I1 torsion angle of 104.1(1)°. The C2,

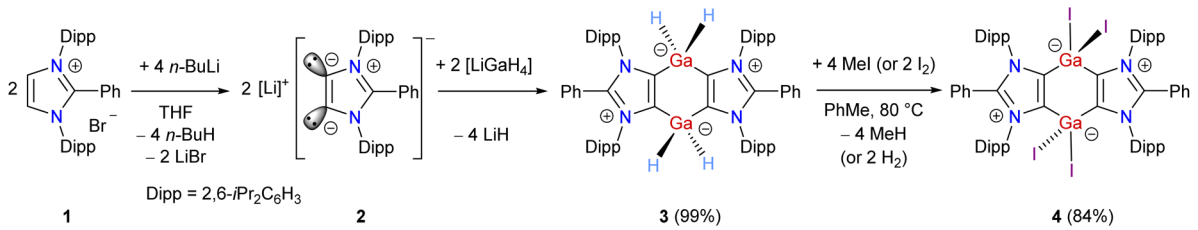

Scheme 1 Synthesis of Ga(III) hydride **3** and iodide **4**.

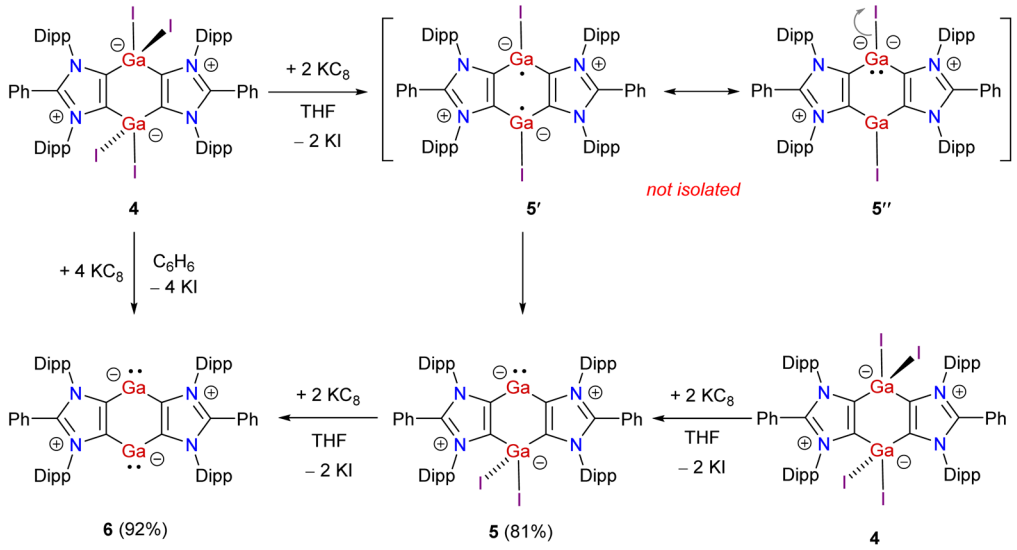

Scheme 2 Synthesis of mixed-valent Ga(I/III) compound **5** and Ga(I) compound **6**.

Ga1, C3′, and I2 atoms are positioned in a semi-trigonal plane with the C3–C2–Ga1–I1 torsion angle of 168.1(1)°.

Having the desired Ga(III) compound **4** in hand, we prompted to perform its reduction. Treatment of **4** with 2 equivalents of KC_8 in THF affords the mixed-valent Ga(I/III) compound **5** as a brown solid in 81% yield (Scheme 2). The exact mechanism of the formation of **5** is currently not known. Direct reduction of one of the Ga(III) atoms of **4** by two equivalents of KC_8 to give **5** is likely. The reduction of **4** to give the putative Ga(II) species **5′**, which may also be viewed as a zwitterionic species **5″**, cannot be ruled out. Finally, the disproportionation of **5′** (*i.e.* formally an intramolecular iodide ion transfer in **5″**) into **5** is calculated to be thermodynamically favored by 17.6 kcal mol^{-1} (see below). Reaction of **4** with 4 equivalents of KC_8 in benzene leads to the clean formation of bis-gallylene **6** as a red-brown solid in 92% yield. **6** can also be prepared by reacting **5** with KC_8. **5** and **6** are crystalline solids, soluble in common organic solvents (THF, toluene, benzene), and stable under an inert atmosphere (of N_2 or Ar) for several weeks. The ^{1}H NMR spectrum of mixed-valent Ga(I/III) compound **5** exhibits four doublets and two septets for the isopropyl groups, suggesting unsymmetrical coordination settings at the Ga atoms. In contrast, the ^{1}H NMR spectrum of bis-gallylene **6** shows two doublets and one septet for the isopropyl groups, which are consistent with the higher symmetry of **6** than **5**. A similar ^{1}H NMR signal pattern is also observed for isostructural compounds featuring Group 14 (ref. 36) or 15 (ref. 25–27) elements in a formally +1 oxidation state. The $^{13}C\{^1H\}$ NMR spectrum of **5** shows two resonances at 163.6 ($CGaI_2$) and 176.4 (CGa) ppm for the C_4Ga_2 moiety. The $^{13}C\{^1H\}$ NMR

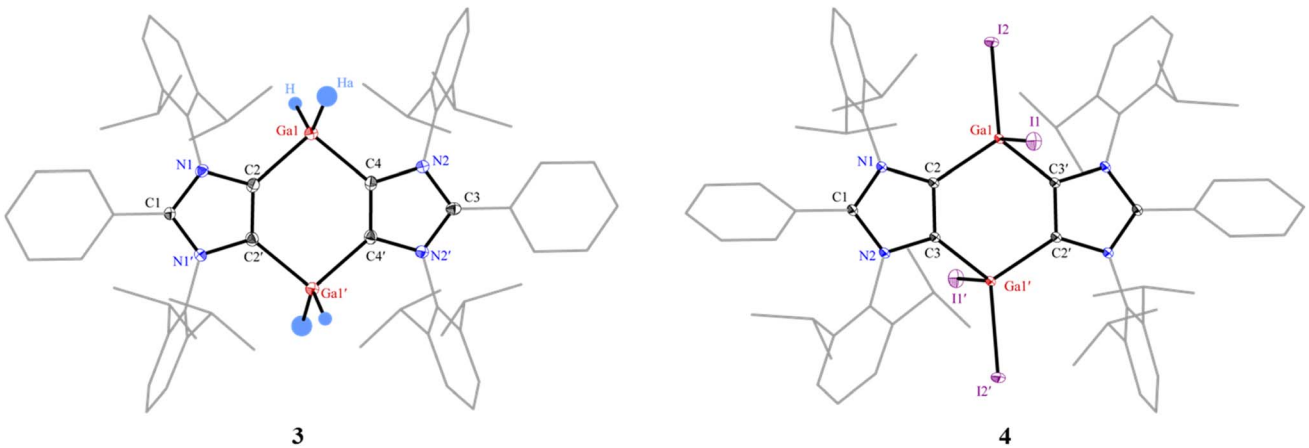

Fig. 2 Solid-state molecular structures of **3** and **4**. Hydrogen atoms (except on GaH_2 for **3**) and two benzene molecules (for **3**) are omitted for clarity. Aryl groups are depicted as wireframes. Thermal displacement ellipsoids at 50%. Selected bond lengths (Å) and angles (°) for **3**: C2–Ga1 2.016(3), C4–Ga1 2.015(3), C2′–C2 1.377(6), C2–Ga1–C4 101.2(1), symmetry code: 2 − *x*, 1 − *y*, *z*; and for **4**: C2–Ga1 1.993(1), C3′–Ga1 1.993(1), Ga1–I1 2.6117(1), Ga1–I2 2.5230(1), C2–C3 1.378(1), I1–Ga1–I2 107.47(1), C2–Ga1–I1 100.14(2), C2–Ga1–I2 117.85(2), C2–Ga1–C3′ 107.36(3), symmetry code: 1 − *x*, 1 − *y*, 1 − *z*.

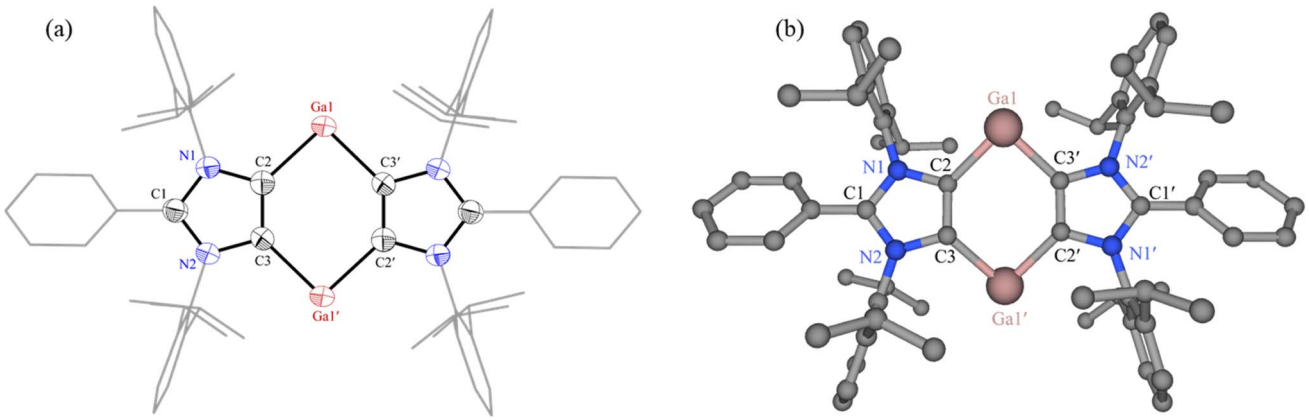

Fig. 3 (a) Solid-state molecular structure of **6**. Only one of two crystallographic independent molecules in the asymmetric unit is shown. Hydrogen atoms, minor disordered parts and solvent molecules were omitted for clarity. Aryl groups are depicted as wireframes. Thermal displacement ellipsoids at 50%. Selected bond lengths (Å) and angles (°): C2–Ga1 2.092(4), C3′–Ga1 2.107(4), C2–C3 1.388(5), C2–Ga1–C3′ 92.6(1), C3–C2–Ga1 132.6(3), symmetry code: $1-x, 1-y, 1-z$. (b) Optimized structure of **6** (r^2SCAN-3c). Selected equilibrium parameters (in Å/°): Ga1–C2 2.128, Ga1–C3′ 2.113, C2–C3 1.393, C2–Ga1–C3′ 91.8.

spectrum of **6** exhibits one signal at 173.6 ppm for the C_4Ga_2 unit.

The solid-state molecular structure of **6** features a planar C_4Ga_2 core embedded between two 1,3-imidazole moieties (Fig. 3a). Compound **6** with two-coordinated Ga(I) atoms may be regarded as a base-stabilized bis-gallylene. Due to the phase transition below 220 K, the reflection data for **6** were collected at 220 K, giving rise to large thermal displacement ellipsoids. The C2–Ga1 (2.092(4) Å) and C3′–Ga1 (2.107(4) Å) bond lengths of **6** are marginally larger than those of Ga(III) compounds **3** (2.016(3) Å) and **4** (1.993(1) Å). The C2–Ga1–C3′ bond angle of **6** (92.6(1)°) is smaller than those of **3** (101.2(1)°) and **4** (107.4(1)°).

To obtain a further insight into the electronic structures of **5** and **6**, we performed quantum chemical calculations at the r^2SCAN-3c level of theory. The optimized molecular structure of **6** is in good agreement with that of sc-XRD structure (Fig. 3). Calculations reveal closed-shell singlet (**CS**) ground state for **5** (Fig. S60†) and **6**. The triplet (**T**) solution for the putative intermediate **5′** (Fig. S61†) is 0.26 kcal mol^{-1} more stable than the **CS** solution. The conversion **5′** → **5** is calculated to be

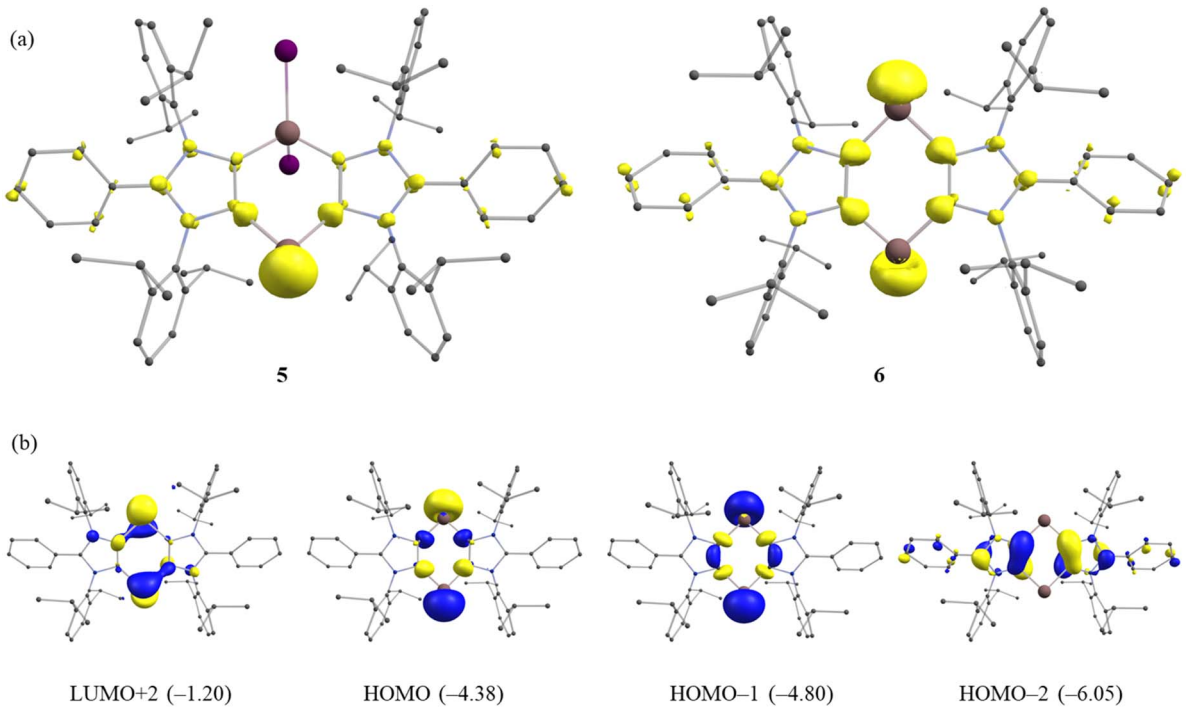

Fig. 4 (a) FOD plots (isosurfaces 0.005) of compounds **5** and **6**. Hydrogen atoms are omitted for clarity. (b) Selected molecular orbitals (0.05) with respective energies (in eV) of **6** according to RKS-PBE0/def2-TZVPP calculations.

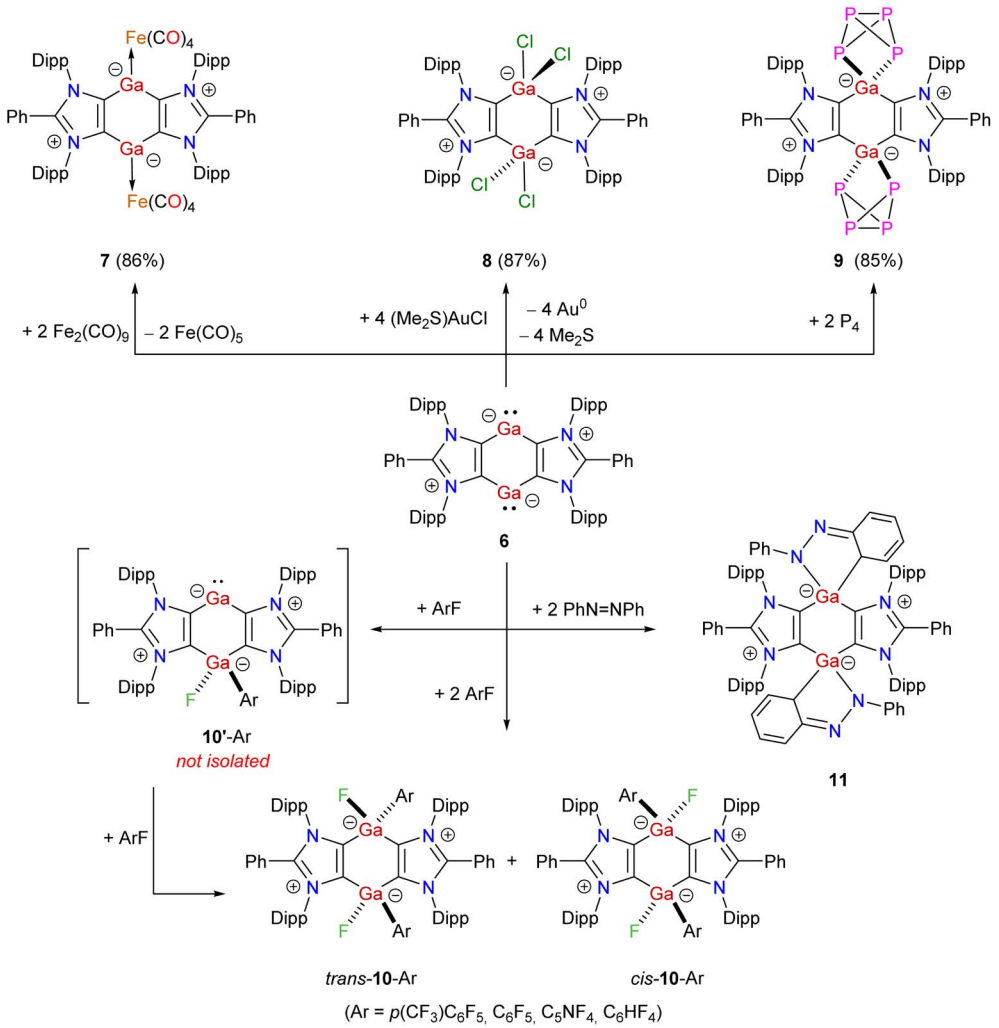

Scheme 3 Room temperature reactivity studies of **6** towards different substrates to **7**–**11**.

thermodynamically favored by 17.6 kcal mol^{-1}. The NBO charges and WBIs (Wiberg Bond Indices) calculated at the PBE0/def2-TZVPP level of theory for **4**, **5**, and **6** (Table S7†) are consistent with their solid-state structures. With the WBIs of 0.45–0.54 and NBO charges of *ca.* −0.32*e* on C atoms, the Ga–C bonds of **4**, **5**, and **6** are essentially polar covalent bonds that are polarized towards the C atoms. The NBO charge(s) on the Ga atom(s) of **4** (1.02), **5** (1.02/0.52), and **6** (0.48) is consistent with its formal (I/III) oxidation state.

We also performed FOD (fractional occupation number weighed density) calculations[37] at the PBE0/def2-TZVPP level of theory to analyze the electron correlation in **5** and **6**. The FOD analyses provide reliable information on the localization of 'hot' (strongly correlated and chemical active) electrons of the molecule.[37] The FOD calculations (PBE0, T = 10 000 K) reveal a moderate level of electron correlation in **5** (N_{FOD} = 2.50 *e*) and **6** (N_{FOD} = 2.85 *e*) (Fig. 4a). The N_{FOD} of **6** is smaller than that of the transient bis-aluminylene **VII** (N_{FOD} = 3.10 *e*).[28]

The HOMO and HOMO−1 of **6** (Fig. 4b) are essentially the electron lone-pairs on the Ga(I) atoms. The LUMO (Fig. S64†) of **6** is based on the ligand, while the LUMO+2 is mainly located on the Ga atoms. The HOMO–LUMO energy gap (ΔE_{H-L}) for **6** amounts to 2.83 eV, which is larger than that of the corresponding fleeting Al(I) species **VII** (1.94 eV).[28] In line with this, the HOMO (Fig. S63†) of mono-gallylene **5** is the lone-pair on Ga(I) atom, while the LUMO+2 is located mainly at the Ga(I) atom. The HOMO of **5** (−4.84 eV) is low-lying than that of **6** (−4.38 eV), suggesting a higher Lewis basicity of the latter. A rather smaller ΔE_{H-L} for **6** (2.83 eV) than **5** (3.18 eV) also implies a greater reactivity of **6**. The UV-Vis spectrum of **5** and **6** each exhibits a main absorption band (λ_{max}) at 300 and 312 nm, respectively (Fig. S48 and S49†). This may be assigned to HOMO−1 → LUMO (**5**) and HOMO−2 → LUMO (**6**) transition.

Treatment of **6** with $Fe_2(CO)_9$ yields the dinuclear Fe(0) complex **7** (Scheme 3). Compound **6** readily oxidizes with (Me_2S)AuCl to yield Ga(III) compound **8** as a colorless solid. Reaction of **6** with white phosphorus affords compound **9** as a brown solid. Prompted by the use of low-valent main-group compounds in the activation of C–F bonds,[38] we performed reactions of **6** with different aryl fluorides (ArF) at room temperature that gave Ga(III) compounds *cis*-/*trans*-**10**-Ar (Ar = *p*-$(CF_3)C_6F_4$, C_6F_5, C_5NF_4, C_6HF_4) as off-white solids. The formation of *cis*-/*trans*-**10**-

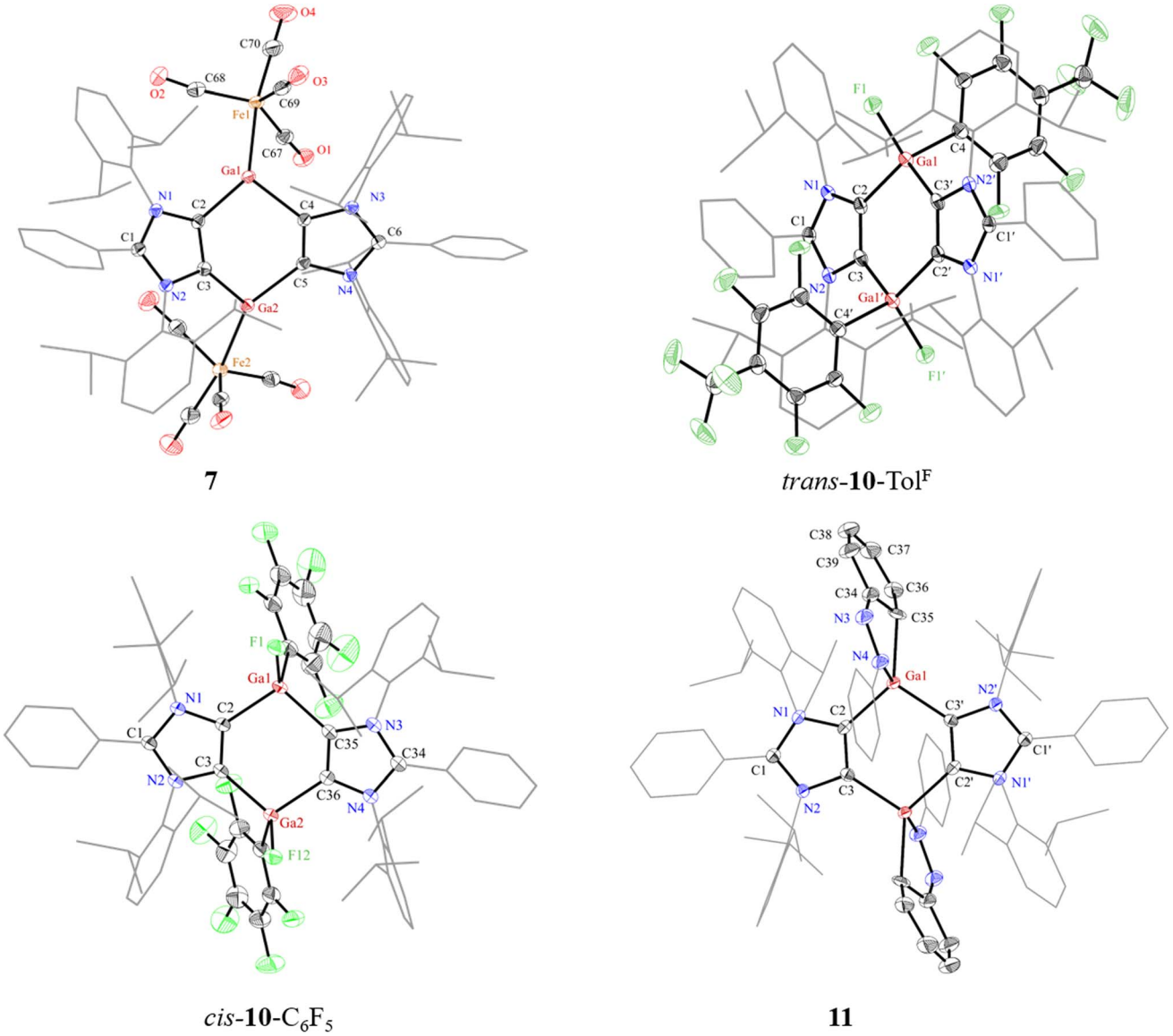

Fig. 5 Solid-state molecular structures of **7**, *trans*-**10**-Tol^F, *cis*-**10**-C_6F_5 and **11**. Hydrogen atoms, minor occupied atoms and solvent molecules were omitted for clarity. Aryl groups (except C_6F_4/C_6F_5 for *trans*-/*cis*-**10**-Ar and N3=C_6H_5 for **11**) are depicted as wireframes. Thermal displacement ellipsoids at 50%. For *trans*-**10**-Tol^F, only one of two crystallographic independent fragments in the asymmetric unit is shown. Selected bond lengths (Å) and angles (°) for **7**: C2–Ga1 2.021(2), C4–Ga1 2.010(2), C3–Ga2 2.009(2), C5–Ga2 2.028(2), Ga1–Fe1 2.327(1), Ga2–Fe2 2.320(1), C2–Ga1–C4 99.9(1), C2–Ga1–Fe1 119.6(1), C4–Ga1–Fe1 139.7(1), C3–Ga2–C5 99.8(1), C3–Ga2–Fe2 139.2(1), C5–Ga2–Fe2 120.3(1); for *trans*-**10**-Tol^F: C2–Ga1 1.997(3), C3′–Ga1 1.997(3), C4–Ga1 2.017(3), Ga1–F1 1.795(2), C2–C3 1.375(4), C2–Ga1–C3′ 106.5(1), symmetry code: $1-x, 1-y, 1-z$; for *cis*-**10**-C_6F_5: C2–Ga1 1.999(1), C35–Ga1 2.003(1), C3–Ga2 1.982(1), Ga1–F1 1.800(1), C2–C3 1.369(2), C2–Ga1–C35 103.8(1); for **11**: C2–Ga1 2.009(2), C3′–Ga1 2.008(2), Ga1–C35 2.052(2), Ga1–N4 1.969(2), N3–N4 1.394(3), N3–C34 1.294(4), C34–C35 1.472(4), C2–Ga1–C3′ 103.8(1), N4–Ga1–C35 82.4(1).

Ar isomers is likely due to the stepwise addition of Ar–F to **6** *via* mixed-valent Ga(I)/Ga(III) species **10′**-Ar. Treatment of **6** with azobenzene at room temperature leads to the [1 + 4]-cycloaddition product **11** in which one of the phenyl rings of azobenzene has dearomatized. The ^{1}H and ^{13}C{^{1}H} NMR spectra of **7**–**11** exhibit expected resonances for the ADC moieties. The ^{13}C{^{1}H} NMR spectrum of **7** features a signal at 216.6 ppm for the carbonyl carbon atoms of the Fe(CO)$_4$ fragments.[39] The ^{1}H NMR spectrum of **8** compares well with that of the related aluminium chloride.[28] The ^{31}P{^{1}H} NMR spectrum of **9** shows two triplets at 152.3 and −298.7 ppm ($^1J_{P-P}$ = 157 Hz), which are consistent with those of a related isostructural P_4-activation product.[40] The ^{19}F{^{1}H} NMR spectra of *cis*-/*trans*-**10**-Ar reveal expected signals for the aryl fluoride moieties as well as a signal for the Ga*F* group in the −205.6 to −207.8 ppm region.[38]

The solid-state molecular structures of **7** (Fig. 5), **8** (Fig. S54†), *trans*-**10**-Tol^F, *cis*-**10**-C_6F_5 (Fig. 5), *trans*-**10**-C_5NF_4 (Fig. S57†), and **11** (Fig. 5) show the expected atom connectivity.[41] The structure of **7** revealed a minor impurity (~3%) with two iodine atoms instead of one Fe(CO)$_4$ group. This is likely

due to the presence of a trace of **5** with **6** used to prepare **7**, which was however not observed in the NMR spectroscopic analysis of the same sample. The sum of the angles at each of three-coordinated Ga atoms of **7** amounts to 359° that is consistent with a trigonal planar coordination environment. The Ga1–Fe1 (2.327(1) Å) and Ga2–Fe2 (2.320(1) Å) bond lengths of **7** are larger than that of [(Cp*Ga)Fe(CO)$_4$] (2.273(1)Å).[39] The four-coordinated Ga atoms of **8**, **9**, *cis*-/*trans*-**10**-Ar, and **11** show a distorted tetrahedral coordination environment. As expected for an oxidized product, the C2–Ga1 (1.997(3) Å) and C3′–Ga1 (1.997(3) Å) bond lengths of *trans*-**10**-Tol^F are smaller than that of **6** (Ga1–C2: 2.092(4) Å), while the Ga1–F1 (1.795(2) Å) bond lengths of *trans*-**10**-Tol^F agree well with other Ga(III) fluorides.[38] A similar trend was shown by *cis*-**10**-C_6F_5 and *trans*-**10**-C_5NF_4. In **11**, the N3–N4 (1.394(3) Å) and C34–C35 (1.472(4) Å) bond lengths are consistent with a single bond,[42] while N3–C34 (1.294(4) Å) bond length corresponds to a C=N double bond.[43] These features show the dearomatization of one of the phenyl groups of azobenzene in **11**.

Conclusions

In conclusion, the first carbocyclic gallylene **5** and bis-gallylene **6** have been reported as crystalline solids. The formation of the mixed-valent Ga(I/III) compound **5** may likely a result of the disproportionation of the transient Ga(II) species **5′**. In addition to the sc-XRD structures of **4** and **6**, electronic structures of **4**, **5**, **5′**, and **6** have been investigated by quantum chemical calculations. Preliminary reactivity studies of **6** have been presented with $Fe_2(CO)_9$ (coordination chemistry), Au(I) chloride (oxidation), white phosphorus (small molecule activation), aryl fluoride (C–F activation), and azobenzene (dearomative cycloaddition) to afford compounds **7**, **8**, **9**, *cis*-/*trans*-**10**-Ar, and **11**, respectively. Further reactivity studies and use of **5** and **6** as ligands as well as substrates for new gallium compounds, in particular aromatic systems and radicals, are expected to add new facets in low-valent gallium chemistry.

Data availability

Experimental details, the plots of NMR, FT-IR, and UV-Vis spectra as well as the detail of X-ray crystallography and theoretical studies of the reported compounds are given in the ESI.† The assigned CCDC identification numbers and the compounds in the study are as follows: CCDC 2334945 (**3**), 2334948 (**4**), 2334949 (**6**), 2334950 (**7**), 2334951 (*trans*-**10**-Tol^F), 2334952 (**8**), 2379059 (*cis*-**10**-C_6F_5), 2379060 (*trans*-**10**-C_5NF_4), and 2334953 (**11**).

Author contributions

AM and SH: experimental investigation, data collection and analysis, writing. YVV: calculations, data collection and analysis, writing. BN and HGS: sc-XRD, data collection and analysis, writing. RSG: conceptualization, investigation, data analysis, writing, editing, supervision. All authors approved the manuscript.

Conflicts of interest

The authors declare no conflict of interest.

Acknowledgements

We are grateful to the Deutsche Forschungsgemeinschaft (DFG) for support [GH 129/16-1 (Project No. 549520861), GH 129/9-1 (Project No. 466111525), GH 129/12-1 (Project No. 514566227); VI 713/3-1 (Project No. 243500032)]. The authors thank Professor Norbert W. Mitzel for his constant encouragement. Arne Merschel thanks Mr Johannes Witte for assistance in starting materials preparation. The HPC facilities at the Universität zu Köln are acknowledged for computing time and programs. Dedicated to Professor Hubert Schmidbaur on the occasion of his 90th birthday.

References

1 A. J. Arduengo, R. L. Harlow and M. Kline, *J. Am. Chem. Soc.*, 1991, **113**, 361–363.
2 (*a*) M. He, C. Hu, R. Wei, X. F. Wang and L. L. Liu, *Chem. Soc. Rev.*, 2024, **53**, 3896–3951; (*b*) M. Asay, C. Jones and M. Driess, *Chem. Rev.*, 2011, **111**, 354–396.
3 (*a*) C. Dohmeier, D. Loos and H. Schnöckel, *Angew. Chem., Int. Ed.*, 1996, **35**, 129–149; (*b*) C. Dohmeier, C. Robl, M. Tacke and H. Schnöckel, *Angew. Chem., Int. Ed.*, 1991, **30**, 564–565; (*c*) D. Loos, E. Baum, A. Ecker, H. Schnöckel and A. J. Downs, *Angew. Chem., Int. Ed.*, 1997, **36**, 860–862.
4 W. Uhl, W. Hiller, M. Layh and W. Schwarz, *Angew. Chem., Int. Ed.*, 1992, **31**, 1364–1366.
5 E. S. Schmidt, A. Jockisch and H. Schmidbaur, *J. Am. Chem. Soc.*, 1999, **121**, 9758–9759.
6 (*a*) M. Zhong, S. Sinhababu and H. W. Roesky, *Dalton Trans.*, 2020, **49**, 1351–1364; (*b*) M. P. Coles and M. J. Evans, *Chem. Commun.*, 2023, **59**, 503–519; (*c*) X. Zhang, Y. Mei and L. L. Liu, *Chem.–Eur. J.*, 2022, **28**, e202202102; (*d*) Y. S. Liu, J. Li, X. L. Ma, Z. Yang and H. W. Roesky, *Coord. Chem. Rev.*, 2018, **374**, 387–415; (*e*) S. Nagendran and H. W. Roesky, *Organometallics*, 2008, **27**, 457–492.
7 C. Cui, H. W. Roesky, H. G. Schmidt, M. Noltemeyer, H. Hao and F. Cimpoesu, *Angew. Chem., Int. Ed.*, 2000, **39**, 4274–4276.
8 N. J. Hardman, B. E. Eichler and P. P. Power, *Chem. Commun.*, 2000, 1991–1992.
9 (*a*) N. Saito, J. Takaya and N. Iwasawa, *Angew. Chem., Int. Ed.*, 2019, **58**, 9998–10002; (*b*) T. Kodama, N. Mukai and M. Tobisu, *Inorg. Chem.*, 2023, **62**, 6554–6559.
10 R. J. Wright, M. Brynda, J. C. Fettinger, A. R. Betzer and P. P. Power, *J. Am. Chem. Soc.*, 2006, **128**, 12498–12509.
11 J. D. Queen, A. Lehmann, J. C. Fettinger, H. M. Tuononen and P. P. Power, *J. Am. Chem. Soc.*, 2020, **142**, 20554–20559.
12 X. Zhang and L. L. Liu, *Angew. Chem., Int. Ed.*, 2021, **60**, 27062–27069.
13 A. Hinz and M. P. Muller, *Chem. Commun.*, 2021, **57**, 12532–12535.

14 (*a*) Q. Yu, L. Zhang, Y. He, J. Pan, H. Li, G.-q. Bian, X. Chen and G. Tan, *Chem. Commun.*, 2021, **57**, 9268–9271; (*b*) H. Li, Y. He, C. Liu and G. Tan, *Dalton Trans.*, 2021, **50**, 12674–12680.

15 S. H. F. Schreiner, T. Rüffer and R. Kretschmer, *Nat. Synth.*, 2024, DOI: **10.1038/s44160-44024-00639-w**.

16 (*a*) G. Feng, K. L. Chan, Z. Lin and M. Yamashita, *J. Am. Chem. Soc.*, 2024, **146**, 7204–7209; (*b*) S. G. Minasian, J. L. Krinsky, J. D. Rinehart, R. Copping, T. Tyliszczak, M. Janousch, D. K. Shuh and J. Arnold, *J. Am. Chem. Soc.*, 2009, **131**, 13767–13783; (*c*) M. Wiecko and P. W. Roesky, *Organometallics*, 2007, **26**, 4846–4848; (*d*) C. Jones, A. Stasch and W. D. Woodul, *Chem. Commun.*, 2009, 113–115; (*e*) D. Dange, C. P. Sindlinger, S. Aldridge and C. Jones, *Chem. Commun.*, 2017, **53**, 149–152; (*f*) R. Y. Kong and M. R. Crimmin, *Dalton Trans.*, 2021, **50**, 7810–7817; (*g*) P. Dabringhaus and I. Krossing, *Chem. Sci.*, 2022, **13**, 12078–12086; (*h*) J. T. Boronski, L. R. Thomas-Hargreaves, M. A. Ellwanger, A. E. Crumpton, J. Hicks, D. F. Bekiş, S. Aldridge and M. R. Buchner, *J. Am. Chem. Soc.*, 2023, **145**, 4408–4413; (*i*) V. A. Dodonov, V. G. Sokolov, E. V. Baranov, A. A. Skatova, W. Xu, Y. Zhao, X.-J. Yang and I. L. Fedushkin, *Inorg. Chem.*, 2022, **61**, 14962–14972.

17 (*a*) J. Kretsch, A. Kreyenschmidt, T. Schillmöller, C. Sindlinger, R. Herbst-Irmer and D. Stalke, *Inorg. Chem.*, 2021, **60**, 7389–7398; (*b*) B. Wang, W. Chen, J. Yang, L. Lu, J. Liu, L. Shen and D. Wu, *Dalton Trans.*, 2023, **52**, 12454–12460; (*c*) D. Dange, S. L. Choong, C. Schenk, A. Stasch and C. Jones, *Dalton Trans.*, 2012, **41**, 9304–9315.

18 (*a*) M. Soleilhavoup and G. Bertrand, *Angew. Chem., Int. Ed.*, 2017, **56**, 10282–10292; (*b*) F. Dahcheh, D. Martin, D. W. Stephan and G. Bertrand, *Angew. Chem., Int. Ed.*, 2014, **53**, 13159–13163; (*c*) R. Kinjo, B. Donnadieu, M. A. Celik, G. Frenking and G. Bertrand, *Science*, 2011, **333**, 610–613; (*d*) C. Pranckevicius, J. O. C. Jimenéz-Halla, M. Kirsch, I. Krummenacher and H. Braunschweig, *J. Am. Chem. Soc.*, 2018, **140**, 10524–10529; (*e*) Y.-J. Lin, W.-C. Liu, Y.-H. Liu, G.-H. Lee, S.-Y. Chien and C.-W. Chiu, *Nat. Commun.*, 2022, **13**, 7051; (*f*) A. D. Ledet and T. W. Hudnall, *Dalton Trans.*, 2016, **45**, 9820–9826; (*g*) M.-A. Légaré, M. Rang, G. Bélanger-Chabot, J. I. Schweizer, I. Krummenacher, R. Bertermann, M. Arrowsmith, M. C. Holthausen and H. Braunschweig, *Science*, 2019, **363**, 1329–1332; (*h*) M.-A. Légaré, G. Bélanger-Chabot, R. D. Dewhurst, E. Welz, I. Krummenacher, B. Engels and H. Braunschweig, *Science*, 2018, **359**, 896–900.

19 X. Zhang and L. L. Liu, *Angew. Chem., Int. Ed.*, 2022, **61**, e202116658.

20 (*a*) P. P. Power, *Organometallics*, 2020, **39**, 4127–4138; (*b*) R. C. Fischer and P. P. Power, *Chem. Rev.*, 2010, **110**, 3877–3923; (*c*) P. P. Power, A. Moezzi, D. C. Pestana, M. A. Petrie, S. C. Shoner and K. M. Waggoner, *Pure Appl. Chem.*, 1991, **63**, 859–866.

21 (*a*) M. L. McCrea-Hendrick, C. A. Caputo, C. J. Roberts, J. C. Fettinger, H. M. Tuononen and P. P. Power, *Organometallics*, 2016, **35**, 579–586; (*b*) Z. Zhu, R. C. Fischer, B. D. Ellis, E. Rivard, W. A. Merrill, M. M. Olmstead, P. P. Power, J. D. Guo, S. Nagase and L. Pu, *Chem.–Eur. J.*, 2009, **15**, 5263–5272; (*c*) N. J. Hardman, R. J. Wright, A. D. Phillips and P. P. Power, *Angew. Chem., Int. Ed.*, 2002, **41**, 2842–2844.

22 Z. Feng, Y. Fang, H. Ruan, Y. Zhao, G. Tan and X. Wang, *Angew. Chem., Int. Ed.*, 2020, **59**, 6769–6774.

23 (*a*) P. Dabringhaus, H. Scherer and I. Krossing, *Nat. Synth.*, 2024, **3**, 732–743; (*b*) A. Barthélemy, H. Scherer, H. Weller and I. Krossing, *Chem. Commun.*, 2023, **59**, 1353–1356; (*c*) A. Barthélemy, H. Scherer, M. Daub, A. Bugnet and I. Krossing, *Angew. Chem., Int. Ed.*, 2023, **62**, e202311648.

24 R. S. Ghadwal, *Angew. Chem., Int. Ed.*, 2023, **62**, e202304665.

25 D. Rottschäfer, B. Neumann, H.-G. Stammler, T. Sergeieva, D. M. Andrada and R. S. Ghadwal, *Chem.–Eur. J.*, 2021, **27**, 3055–3064.

26 D. Rottschäfer, T. Glodde, B. Neumann, H.-G. Stammler, D. M. Andrada and R. S. Ghadwal, *Angew. Chem., Int. Ed.*, 2021, **60**, 15849–15853.

27 H. Steffenfauseweh, D. Rottschäfer, Y. V. Vishnevskiy, B. Neumann, H.-G. Stammler, D. W. Szczepanik and R. S. Ghadwal, *Angew. Chem., Int. Ed.*, 2023, **62**, e202216003.

28 A. Merschel, Y. Vishnevskiy, B. Neumann, G. Stammler and R. Ghadwal, *Chem.–Eur. J.*, 2024, **30**, e202400293.

29 D. Rottschäfer, F. Ebeler, T. Strothmann, B. Neumann, H.-G. Stammler, A. Mix and R. S. Ghadwal, *Chem.–Eur. J.*, 2018, **24**, 3716–3720.

30 (*a*) D. Rottschäfer, B. Neumann, H.-G. Stammler, M. v. Gastel, D. M. Andrada and R. S. Ghadwal, *Angew. Chem., Int. Ed.*, 2018, **57**, 4765–4768; (*b*) N. K. T. Ho, B. Neumann, H.-G. Stammler, V. H. Menezes da Silva, D. G. Watanabe, A. A. C. Braga and R. S. Ghadwal, *Dalton Trans.*, 2017, **46**, 12027–12031.

31 A. Merschel, Y. V. Vishnevskiy, B. Neumann, H.-G. Stammler and R. S. Ghadwal, *Chem.–Eur. J.*, 2023, **29**, e202301037.

32 (*a*) M. D. Francis, D. E. Hibbs, M. B. Hursthouse, C. Jones and N. A. Smithies, *J. Chem. Soc., Dalton Trans.*, 1998, 3249–3254; (*b*) A. Hock, L. Werner, C. Luz and U. Radius, *Dalton Trans.*, 2020, **49**, 11108–11119.

33 X. Wang and L. Andrews, *J. Phys. Chem. A*, 2003, **107**, 11371–11379.

34 See the data availability section.

35 (*a*) A. Merschel, Y. V. Vishnevskiy, B. Neumann, H. G. Stammler and R. S. Ghadwal, *Angew. Chem., Int. Ed.*, 2024, **63**, e202318525; (*b*) A. Merschel, T. Glodde, B. Neumann, H.-G. Stammler and R. S. Ghadwal, *Angew. Chem., Int. Ed.*, 2021, **60**, 2969–2973; (*c*) A. Merschel, D. Rottschäfer, B. Neumann, H.-G. Stammler and R. S. Ghadwal, *Organometallics*, 2020, **39**, 1719–1729.

36 (*a*) M. K. Sharma, F. Ebeler, T. Glodde, B. Neumann, H.-G. Stammler and R. S. Ghadwal, *J. Am. Chem. Soc.*, 2021, **143**, 121–125; (*b*) M. K. Sharma, D. Rottschäfer, T. Glodde, B. Neumann, H. G. Stammler and R. S. Ghadwal, *Angew. Chem., Int. Ed.*, 2021, **60**, 6414–6418; (*c*) F. Ebeler, Y. V. Vishnevskiy, B. Neumann, H. G. Stammler, D. W. Szczepanik and R. S. Ghadwal, *J. Am. Chem. Soc.*, 2024, **146**, 30584–30595.

37 (*a*) C. A. Bauer, A. Hansen and S. Grimme, *Chem.–Eur. J.*, 2017, **23**, 6150–6164; (*b*) S. Grimme and A. Hansen, *Angew. Chem., Int. Ed.*, 2015, **54**, 12308–12313.
38 (*a*) O. Kysliak, H. Görls and R. Kretschmer, *J. Am. Chem. Soc.*, 2021, **143**, 142–148; (*b*) M. R. Crimmin, M. J. Butler and A. J. White, *Chem. Commun.*, 2015, **51**, 15994–15996.
39 P. Jutzi, B. Neumann, G. Reumann and H.-G. Stammler, *Organometallics*, 1998, **17**, 1305–1314.
40 (*a*) G. Prabusankar, A. Doddi, C. Gemel, M. Winter and R. A. Fischer, *Inorg. Chem.*, 2010, **49**, 7976–7980; (*b*) M. Scheer, G. Balázs and A. Seitz, *Chem. Rev.*, 2010, **110**, 4236–4256.
41 For **9**, the proposed structural motif was ascertained by preliminary X-ray diffraction outcomes, unfortunately poor diffracting nature of crystals resulted in an unpublishable data set.
42 P. Pyykkö and M. Atsumi, *Chem.–Eur. J.*, 2009, **15**, 186–197.
43 P. Pyykkö and M. Atsumi, *Chem.–Eur. J.*, 2009, **15**, 12770–12779.